Correlating yield response with molecular architecture in polymer glasses

Kevin J. Calzia · Alan J. Lesser

Abstract The yield response of nine architecturally different glassy networks is investigated under several stress states, strain rates, and temperatures, and correlations are made among them. Differences in molecular architecture are quantified through two proposed governing parameters; the glass transition temperature, T_g, capturing network stiffness and the cohesive energy density, E_c, reflecting network strength. Cohesive energy density is estimated using molecular modeling techniques and supported by solvent swelling experiments. The limits of the correlations made between molecular architecture and yield behavior are further studied with attempts to relate yielding in thermoplastic glasses and heterogeneous networks.

Introduction

There is a significant amount of research focused on glassy polymers and specifically epoxy thermosets. This is understandable since approximately 603 million pounds of epoxy resin are produced annually in North America alone [1]. These resins are used in applications ranging from coatings and adhesives to composite matrices. An important feature of epoxy thermosets allowing them to be used in so many applications is the wide variety of chemistries available. With so many

variations, formulators are able to tailor characteristics for a particular application. The number of applications that epoxy thermosets are used in is increasing, and with this, an even greater variety of chemistries are available. It has become an increasingly difficult task to select a proper formulation and predict how it will perform under specific conditions. Subtle changes in chemistry can produce drastic changes in mechanical behavior when used under different stress states, temperatures, and loading rates. Consequently, introducing new products into the marketplace or altering existing products by formulation changes usually requires an extensive experimental test program. These programs are so expensive and time-consuming that formulations are only optimized in selected cases. Alternate methods are critical to estimate mechanical properties of resins from their molecular architecture. The ability to predict specific engineering properties in polymer glasses from characteristics of their molecular and chemical architecture is of great interest.

Considerable research has previously been done to relate the underlying physical characteristics of glassy polymers to their mechanical behavior in certain applications [2–7]. Several studies have attempted to correlate specific mechanical behavior, such as crazing, with physical parameters [8, 9]. Relationships have been proposed between properties such as the tensile and shear modulus and crazing characteristics [8]. However, no correlations have been made with parameters that reflect differences in the molecular architecture of the material. Since these models lack fundamental information about the structure and chemical makeup of the polymer, they are often valid for only one specific system or generalizations regarding material response can only be made.

K. J. Calzia · A. J. Lesser (✉)
Polymer Science and Engineering Department, University of Massachusetts Amherst, 120 Governors Dr, Amherst, MA 01003, USA
e-mail: ajl@polysci.umass.edu

Molecular simulations have been utilized to model both yield and elastic characteristics of polymer glasses. Early simulations have been successful at modeling relatively simple stress states and test conditions on ideal polymer chains [10, 11]. More recent modeling has also been performed on systems under complex stress states and unique geometries [12]. Other studies have attempted to predict the elastic constants from simulated deformations [13]. All of these simulations consider specific polymer systems, but contain few or no molecular details. These simulations agreed with earlier, simpler models, but parameters that indicate how alterations in chemistry or structure govern the yield behavior are not identified. There are only general conclusions that can be made from the work in these simulations.

An alternate approach is to correlate specific engineering properties with physical characteristics that can be predicted using recent molecular modeling techniques. The basis of this approach relies on the fact that not all physical and mechanical properties are independent of one another. Most can be related in one way or another to molecular structure and processing conditions. For example, it is well established that the yield stress is inversely associated with the fracture toughness of a material [5, 14]. In this paper, it is shown how the yield stress of a glassy polymer is highly correlated to two of its physical properties. These properties include the glass transition temperature, T_g, which reflects the network stiffness of the glass, and the cohesive energy density, E_c, which describes the relative strength of the glassy network. These two parameters are found to also be greatly affected by changes in molecular structure. These changes can be relatively easily quantified with measurements using small sample sizes and predictions made through molecular simulations.

Experimental and numerical methods

Materials

A range of formulations was chosen to investigate the effects of T_g and E_c on the yield behavior of polymer glasses. The first five formulations were all based on a bisphenol-A diglycidyl ether epoxy resin. Two of these systems were cured with aliphatic and aromatic amines and will be referred to as the aliphatic and aromatic model systems. The other three epoxy-based formulations are different in that they utilized bisphenol-A based compounds as chain extenders and are crosslinked with a tetrafunctional amine or a trifunctional phenolic compound. These systems will be referred to as the phenolic extended systems due to the unique chain extender used with them.

Two thermoplastic glasses, polycarbonate and polystyrene, were selected for comparison with the thermosetting materials. Six additional systems reported in the literature are introduced for further comparison and were all crosslinked networks. The specific chemistries and architectures of all the above systems are explained in detail in the following paragraphs.

The aliphatic and aromatic model systems were formulated using Epon 825, a diglycidyl ether of bisphenol-A supplied by Resource Resins Inc. The aliphatic system consisted of ethylene diamine (EDA) as a crosslinker and N,N′-dimethylethylenediamine (DMEDA) as a chain extender both purchased from Aldrich and used without further purification and shown in Table 1. By adjusting the ratio of these two monomers, various crosslink densities or molecular weights between crosslinks, M_c, could be achieved. The aromatic system was formulated using 1,3-phenylenediamine (mPDA) as a crosslinker and aniline as a chain extender, again both were purchased from Aldrich and used without further purification.
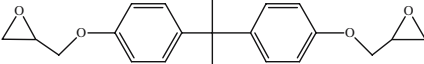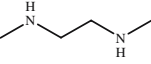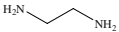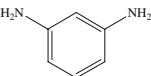
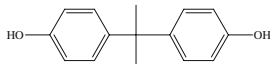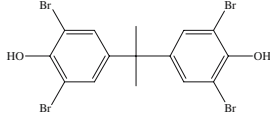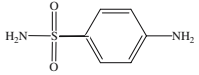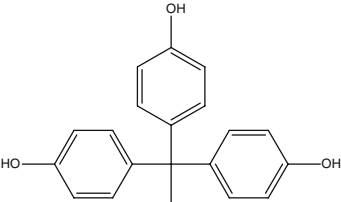The three phenolic extended epoxy systems were formulated using DER 332, bisphenol-A diglycidyl ether (BADGE) supplied by Dow Chemical. They utilized bisphenol-A (BA) or tetrabromobisphenol-A (TBBA) as chain extenders whose structures are shown in Table 1. Two of the formulations were crosslinked with sulfanilamide (SA) while a third formulation used tris(4-hydroxy phenyl) ethane (THPE) as a crosslinker and BA as a chain extender. Approximately 100 μL of triphenylethylphosphonium acetate (60% in methanol), or A-1 catalyst, was added per 100 g of total monomer to catalyze the phenol/epoxide ring reaction. The BADGE, BA, TBBA, and A-1 catalyst were all used as received from Dow Chemical. The SA and THPE were purchased from Aldrich and used in their as received condition too.

Makrolon 3208 polycarbonate (PC) was supplied by Bayer and used for comparison. Polystyrene (PS) with a M_n of 45,000 g/mol was purchased from Aldrich and used as received.

Sample preparation

Water was removed from the Epon 825 by placing the resin in a vacuum oven at 80 °C for 12 h and was stored at 50 °C thereafter. Amines were added in stoichiometric quantities to achieve precise M_c values and blended with the resin. All mixing of the resin and curatives was done at room temperature with exception

Table 1 Structures of monomers used for the aliphatic and aromatic systems as well as the phenolic extended networks

Monomer	Molecular Weight (g/mol)
epoxy resin (DER 332 or Epon 825)	350 or 352
N,N'-dimethylethylenediamine	88.15
ethylenediamine	60.1
aniline	93.13
1,3-phenylenediamine	108.14
bisphenol-A	228
tetrabromobisphenol-A	544
Sulfanilamide	172.21
tris (4-hydroxyphenyl) ethane	306

of mPDA being melted at 80 °C before mixing. The amines were thoroughly mixed with the resin for approximately 2 min and then placed at 50 °C for 3 min for degassing. Compression bullets were cast in 11.5 mm diameter test tubes pretreated with a mold release, SurfaSil (Pierce Chemical), to ease removal. Plaques were cast between two glass plates treated with a mold release and separated by a 3 mm teflon spacer. The resin was cured at 50 °C for 3–12 h with the longer cure times used on the slower reacting aromatic systems. A post-cure followed at 20 °C above the highest measured T_g of the systems for 3 h to insure complete conversion. Compression bullets were cut from the cured cylinders with a diamond saw in 23 mm lengths.

The phenolic extended systems were prepared by heating the DER 332 to 150 °C while stirring in a round bottom flask. The chain extender was then added and allowed to dissolve. The mixture was cooled to 140 °C and the crosslinker was added with further cooling to near 130 °C. The catalyst was then quickly added and stirred for 30 s. The mixture was poured between two glass plates treated with a mold release and cured for 3 h at 200 °C to make a 3 mm plaque. From this plaque, plane strain test samples were machined.

Polycarbonate compression bullets were compression molded in a cylindrical mold at 250 °C for 15 min. The PC pellets were dried at 50 °C in a vacuum oven prior to molding. Polystyrene compression bullets were cast in 11.5 mm test tubes at 280 °C for 30 min.

Mechanical testing

Uniaxial compression tests were conducted on a Model 1123 Instron at a variety of temperatures specified in the discussion and at an axial strain rate of 0.1 min^{-1} equivalent to an octahedral strain rate of 0.043 min^{-1}. The phenolic extended systems were tested in plane strain at 25 °C and an axial strain rate of 0.02 min^{-1}. The region in the nominal stress versus strain curve where the slope reaches zero was defined as the compressive yield stress. A more conservative method for determining the yield stress may also be used, giving a lower yield value than what is reported here. However, the overall correlations shown between yield and the identified molecular parameters would not change regardless of the method used.

Density measurements

The physical density of the cured resins was measured using the water buoyancy method described in ASTM D-792. Square samples measuring 25 mm by 25 mm and 3 mm in thickness were used for the measurement.

Cohesive energy density estimations

Cohesive energy density, E_c, was estimated using Accelrys' Materials Studio program. Short segments of an epoxy network containing six repeat units were used for the aliphatic and aromatic systems with each repeat consisting of a bisphenol-A epoxy molecule ring opened by a chain extender or crosslinking monomer. Crosslink junctions were represented as one repeat growing off the previously reacted units and another repeat continuing down the chain. A range of M_c values were modeled by altering the ratio of chain extender and crosslinking molecules present in the repeat length. A minimization was performed to find the lowest energy state from which an amorphous cell was constructed. The amorphous cell construction created a representative volume of material dependent upon the input temperature and density of the system being modeled. A dynamic simulation was run on the amorphous cell at 298 K and E_c was calculated from the three lowest energy conformations. The COMPASS force field was imposed for the systems during minimization and simulation runs. Calculations with comparison systems taken from literature were performed in a similar fashion with a six repeat length used during modeling. An eight repeat length was used for modeling the three phenolic extended systems. A repeat length was defined in the same way as above for the aliphatic and aromatic systems.

Swelling experiments

Equilibrium mass uptake values were determined from 25 mm by 25 mm squares cut from 3 mm plaques. The samples were placed in a sealed jar with 30 ml of solvent and mass values were recorded over time. Mass readings were made after lightly wiping each side of the sample. A variety of solvents consisting of hexane, cyclohexane, carbon tetrachloride, toluene, tetrahydrofuran, methyl ethyl ketone, chloroform, acetone, and propanol were chosen because of their solubility parameters. All of them were purchased from Aldrich and used without purification.

Results and discussion

Identification of molecular parameters

Earlier research conducted in this laboratory and others has shown the crosslink functionality, f_c, molecular weight between crosslinks, M_c, and backbone stiffness all contribute to the glass transition temperature, T_g, of

a crosslinked glassy network [15–18]. Differences in f_c and M_c represent changes in molecular architecture while changing from aliphatic to aromatic curatives represents changes in the chemical architecture of the network. By changing the chemical structure and architecture of the network, backbone stiffness is altered. Since T_g is affected by changes in both architecture and chemistry and these factors change the stiffness of the network, T_g is considered to be a physical parameter that reflects overall network stiffness.

The yield response of a thermoset is also affected by its T_g. As T_g increases, the yield stress generally increases for a given system [15, 16]. If one introduces the effects of temperature, the yield stress of a high T_g network tested at a high temperature will appear to be comparable to a low T_g network tested at a lower temperature. Thus, yield in glassy networks can be compared by shifts in test temperature and selecting T_g as a reference temperature. One must remember though that a change in T_g represents a difference in the actual molecular architecture of the network and a shift in temperature is only a change in the surrounding test environment. Going one step beyond shifting with temperature, plots constructed of yield stress versus a normalized parameter of test temperature over T_g, T/T_g, helps to correlate yield behavior and network stiffness of an aliphatic and aromatic amine cured epoxy as shown in Fig. 1 [19–21]. One notices within the aliphatic and aromatic systems the data does tighten up slightly, but not perfectly well. If the two plots were superimposed on the same graph, two different trends would be seen for each network. Once the chemical architecture, changing from aliphatic to aromatic amine curatives, of a system changes the yield response scales differently with T_g and shifting with temperature is not enough for comparisons between networks [15, 16, 19–21]. This suggests that T_g alone is insufficient to account for differences in molecular architecture and additional parameters are needed to relate changes in architecture, chemistry, and yield behavior.

Consequently, cohesive energy density, E_c, is chosen as an additional parameter to accommodate changes in molecular architecture. From a molecular perspective, since T_g describes network stiffness, it would seem logical that another parameter describing network strength would be complimentary to T_g and aid in understanding yield at the molecular level. In fact, a good physical definition of E_c is a measurement of the internal forces binding a substance together or its cohesive, network strength. Also, E_c has units of energy per volume, which from a more continuum perspective correlates nicely with several earlier yield models. The modified von Mises equation proposed by
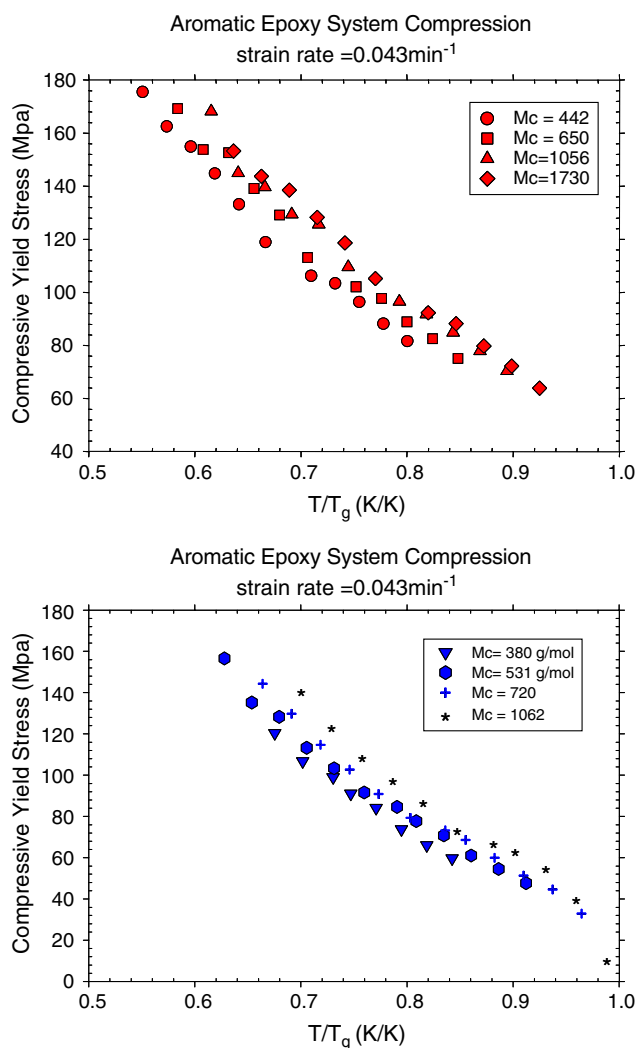
Fig. 1 The compressive yield stress is correlated with network stiffness through a normalized parameter T/T_g for the (**a**) aromatic and (**b**) aliphatic networks over a range of temperatures

Sternstein [2] and others requires a critical distortional energy density needed for yielding to occur. Models proposed by Robertson [6] and Ward [7] possess activation energies and volumes giving energy density terms that describe specific energetic requirements needed for yielding. Since E_c is an energy density value, it is reasoned that it would be an ideal physical property having a significant effect on yield.

Estimating cohesive energy density

Although accurate measurements of E_c are often difficult, it can be estimated using molecular simulations. Summation techniques have been shown to work reasonably well for small molecule compounds, but this can become quite tedious for large macromolecules and it does not always consider all the specific

interactions of a polymer chain folding upon itself and in the case of thermosets, the additional interactions provided by the crosslinks [22]. Thus, for our correlations E_c was estimated using Accelrys' Materials Studio molecular modeling program.

Lengths of eight repeat units were used for all of the systems with the exception of eight units used for the phenolic extended systems. These lengths allowed for enough variation in the crosslink junction to chain extended region ratio to achieve the variety of crosslink densities chosen for mechanical testing. These repeat lengths also gave a simulated amorphous cell of 500–1000 atoms in general which is considered to be an acceptable size [23]. It was found E_c would increase as the repeat length increased, but problems began to arise in the simulation itself at greater lengths. At around 12 repeat units, the simulation would fail due to an excessive number of atoms present causing aromatic ring catenations or long computation times on the order of 1 day. So the repeat length was kept at 6 and 8 units for the model systems.

The physical density of the glass increases as crosslink density of the network increases as shown in Fig. 2. Though the changes in physical density are subtle, they have a significant effect on the estimated E_c. This is expected since as the network becomes more dense, the interactions between the polymer chains themselves change, thereby altering E_c. Therefore, the simulations were performed using the measured density of each network giving a more representative estimate of E_c for each particular network. In addition, using relatively long equilibration and simulation times of 10^6 fs further refined the simulation technique. Initial simulations were conducted with shorter times. By increasing the simulation time the final energy state tended to be more stable and reproducible. Therefore, it is believed the longer simulation times are more representative of the
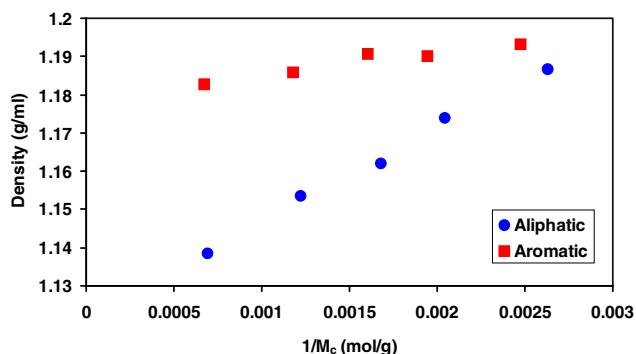
amorphous cell being in equilibrium. Each simulation was also performed several times and the results were averaged for improved accuracy.

Figure 3 shows E_c plotted versus $1/M_c$, or crosslink density, for the aliphatic and aromatic systems. Each data point represents an average of multiple simulations performed at each crosslink density. There are two trends apparent in the plot; one is the aliphatic networks appear to have a slightly greater E_c than the aromatic systems which might not be expected from looking at the functional groups present in the network. The other trend is E_c increases with decreasing crosslink density or increasing M_c. Also note E_c for these two systems is in the range of 300–400 MJ/m^3.

To experimentally validate the estimated values of E_c, equilibrium swelling experiments were conducted. By measuring the mass uptake of the cured epoxy resin with a variety of solvents possessing a range of solubilities, the solvent that provides the greatest mass uptake should have the most similar solubility parameter as the cured resin. The solubility parameter squared is equivalent to E_c so the solvent providing the greatest mass uptake also must have the most similar E_c [22]. The results of these experiments are shown in Table 2. It took up to 3 weeks for equilibrium to be obtained in some network-solvent combinations. For the networks that were tested general agreement is
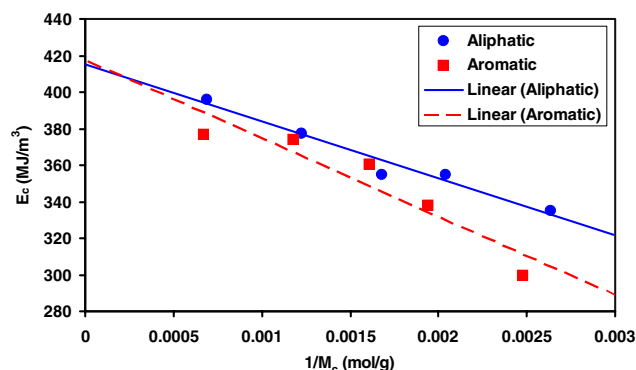
Fig. 3 Trends of E_c and $1/M_c$ for the aliphatic and aromatic systems

Table 2 E_c as determined from molecular modeling simulation techniques and equilibrium mass uptake swelling experiments

Network	E_c (MJ/m^3) as determined from	
	Simulation	Swelling
Aliphatic M_c 950	380	375
Aliphatic M_c 1452	396	373
Aromatic M_c 850	374	374
Aromatic M_c 1489	377	375

Fig. 2 Density of the cured network increases with increasing crosslink density for both the aliphatic and aromatic systems

seen between the estimated E_c values from simulations and those determined from swelling experiments. Though the swelling experiments do not support the trends reported from simulations, the values are in general agreement.

Correlating yield with T_g and E_c

Figure 1 collects the effects of network stiffness, described by T_g, in one normalized term. To incorporate the effects of network strength, measured by E_c, a modified von Mises yield model is proposed. This model, as described below, captures not only changes in strain rate, test temperature, and stress state, but also considers molecular architecture. When discussing yield across a range of stress states it is often easier to work in terms of the octahedral shear stress as defined below in Eq. 1.

$$\tau^{\text{oct}} = \frac{1}{3}\sqrt{(\sigma_1 - \sigma_2)^2 + (\sigma_1 - \sigma_3)^2 + (\sigma_2 - \sigma_3)^2} = \sqrt{\frac{2}{3}J_2} \tag{1}$$

where τ^{oct} is the octahedral shear stress, σ_1, σ_2, and σ_3 are the principal stresses, and J_2 is the second invariant of the deviatoric stress tensor. The yield behavior of polymers is affected by stress state, and if temperature and strain rate are held constant, it can be described by a modified von Mises yield criteria [2] written in Eq. 2.

$$\tau_y^{\text{oct}} = \tau_{y0}^{\text{oct}} - \mu\sigma_m \tag{2}$$

where τ_y^{oct} is the octahedral shear yield stress, τ_{yo}^{oct} is the octahedral shear yield stress in the absence of hydrostatic or mean stress, σ_m, and μ is the coefficient of internal friction. The mean stress is also related to the first invariant of the stress tensor, I_1, and the normal stresses, σ_{ii}, described by Eq. 3.

$$\sigma_m = \frac{1}{3}I_1 = \frac{1}{3}\sigma_{ii} \tag{3}$$

Many others have demonstrated that, if the stress state is held constant while systematically varying the strain rate and temperature, these materials follow an Erying-type stress-induced, thermally-activated yield response as proposed by Robertson [6] and later by Ward [7]. More recent studies by Kody [24] have shown that if Ward's model is applied to the octahedral plane, the yield response can be expressed in the form of Eq. 2 with the respective parameters taking the form of Eq. 4.

$$\tau_{y0}^{\text{oct}} = \frac{E}{\nu} + \frac{RT}{\nu}\ln\left(\frac{\dot{\gamma}^{\text{oct}}}{\Gamma}\right) \tag{4}$$
$$\mu = \Omega/\nu$$

where E is the activation energy, ν and Ω are the activation volumes for pure shear deformation (distortion) and pure dilatation, respectively, $\dot{\gamma}^{\text{oct}}$ is the octahedral strain rate, R is the gas constant, T is the temperature, and Γ is a proportionality constant. In later reports by Lesser [19], Eq. 4 was modified to incorporate the effects of network stiffness, T_g, and network strength, E_c, to give Eq. 5.

$$\hat{\tau} = \frac{E}{\nu E_c} + \frac{RT_g}{\nu E_c}\ln\left(\frac{\dot{\gamma}^{\text{oct}}}{\Gamma}\right)\hat{T} - (\Omega/\nu)\hat{\sigma}_m \tag{5}$$

where the terms are defined as

$$\hat{\tau} = \tau_y^{oct}/E_c$$
$$\hat{T} = T/T_g \tag{6}$$
$$\hat{\sigma}_m = \sigma_m/E_c$$

Eq. 5, with the terms defined as in Eq. 6, is the proposed yield model that incorporates the effects of changing molecular architecture. The yield behavior of several glassy networks with various molecular architectures will be correlated following these equations.

If stress state and strain rate are held constant, a plot of τ_y^{oct}/E_c versus T/T_g should relate network stiffness and strength to the yield response of a resin in a linear fashion as predicted by Eq. 5. Figure 4 shows a correlation between yield stress and molecular parameters for the aliphatic and aromatic systems tested in
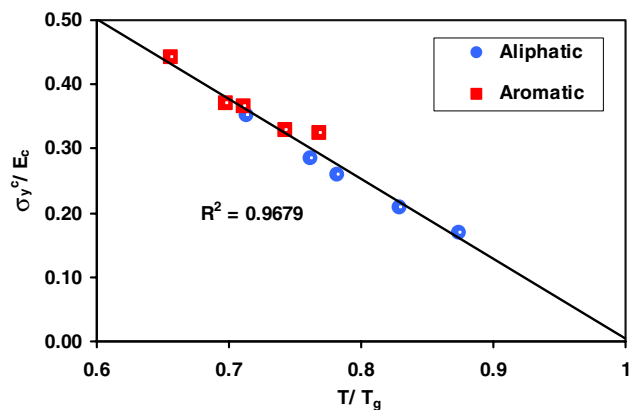
Fig. 4 The compressive yield stress normalized by E_c and plotted versus T/T_g for the aliphatic and aromatic networks. Regardless of molecular architecture the networks collapse onto a single line. Tests performed at 298 K and 0.1 min^{-1}
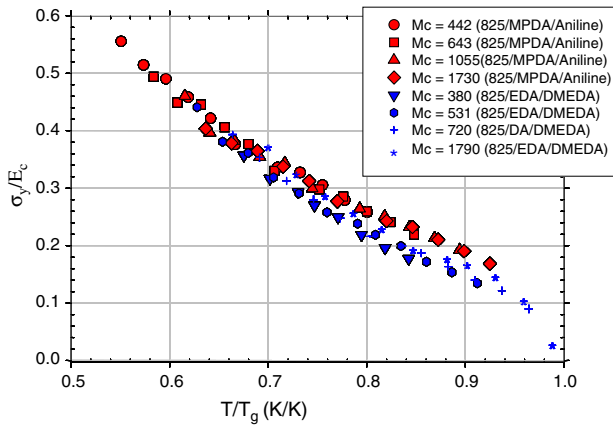
Fig. 5 The aliphatic and aromatic systems tested in uniaxial compression at a strain rate of 0.1 min^{-1} across a range of temperatures still collapse linearly

uniaxial compression. Note that $\sigma_y^c = 3/\sqrt{2}\tau_y^{oct}$ where σ_y^c is the yield stress measured in uniaxial compression.

With the two normalized axes presented in Fig. 4, it becomes clear, regardless of molecular structure along the backbone, the yield response of both the aliphatic and aromatic systems collapse onto a single line. The yield behavior of two architecturally different epoxy networks has now been related through two molecular parameters, T_g and E_c capturing the effects of network stiffness and strength, respectively. The fact the data plots in a linear manner also suggests Eq. 5 is of the proper form.

To investigate the generality of T_g and E_c as molecular parameters, the compressive yield stress of the aliphatic and aromatic networks was measured over a range of temperatures. An identical plot as just

shown, with two normalized axes, is constructed and a similar collapse of the data is seen in Fig. 5. As the test temperature approaches the T_g of each material, the trendline begins to separate. This may be due to other molecular motions occurring that are not captured with T_g or E_c since E_c was calculated at 25 °C and not at higher temperatures. However, within a given system the data still collapses at these temperatures.

In Figs. 4 and 5, yield was correlated with network stiffness and strength considering a single stress state and various test temperatures. The aliphatic and aromatic networks were also tested under various stress states ranging from uniaxial compression to pure shear to uniaxial tension to equi-biaxial tension. The details of these tests utilizing specially fabricated hollow cylinders can be found elsewhere [24]. If a third axis is plotted containing mean stress, changes in stress state can be accounted for. Hence a 3-D plot of τ_y^{oct}/E_c versus σ_m/E_c versus T/T_g is constructed and shown in Fig. 6 with two different views. The first view 6a shows changes in stress state and one sees as a greater hydrostatic stress is applied to the sample, the octahedral shear yield stress decreases. If one looks at a single stress state in this view, i.e., at a given σ_m/E_c value, one can see that octahedral shear yield stress decreases with increasing test temperature. All of the data is fit by linear regression with a single plane. Figure 6b clearly shows the data from both the aliphatic and aromatic networks lie upon this plane with an r^2 value of 0.9704.

Additional architectures were also investigated to evaluate the correlations suggested from the model systems. These include phenolic extended systems where the backbone stiffness is altered by the addition
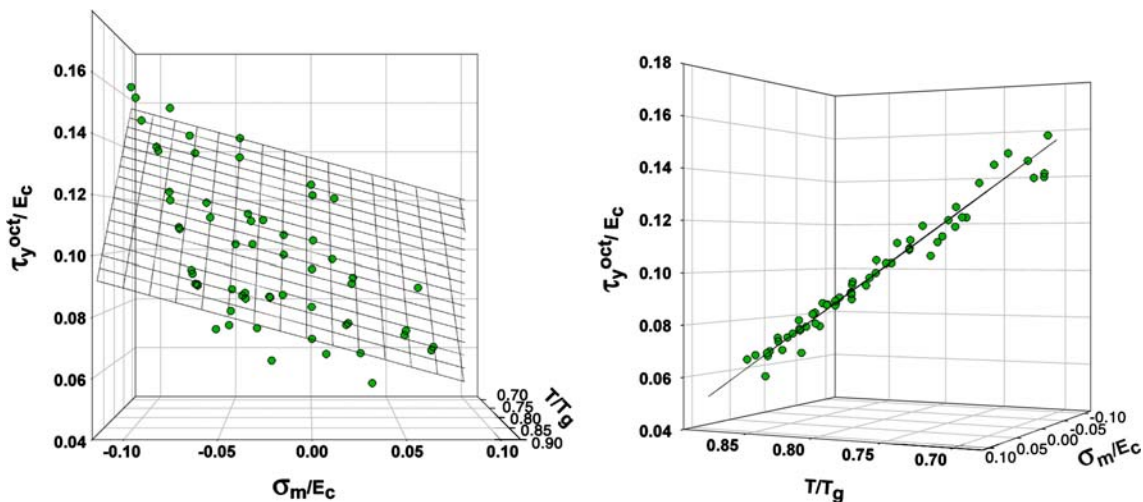

Fig. 6 Both the aliphatic and aromatic networks collapse onto a single plane when the effects of stress state are considered and introduced as a third axes through σ_m/E_c. Tests performed at an octahedral strain rate of 0.043 min^{-1}

of large pendant bromine groups and in addition crosslink functionality is changed by using a tri-functional epoxy. The changes in molecular architecture can be seen in the structure of each monomer shown in Table 1. These phenolic extended systems were prepared, tested in plane strain, and their T_g and E_c values determined. The data is normalized as before and a collapse is seen among the systems shown in Fig. 7. This further suggests T_g and E_c are effectively capturing network stiffness and strength as significant changes have been made in the molecular architecture and yield behavior can still be correlated.

Similar correlations are observed with four polymers selected from literature. These systems are selected upon their differences in molecular structure from the model systems and the required data being reported for collapse of the yield response and modeling. All systems chosen are tested in axial compression, but at various strain rates with a correctional shift following a logarithmic ratio of the actual $\dot{\gamma}^{oct}$ over a reference $\dot{\gamma}^{oct}$ of the model systems. The systems are a bismaleimide (BMI) [25], a trifunctional and bisphenol-A epoxy cured with diaminodiphenyl sulfone (DDS) [26], a bisphenol-A epoxy cured with amines containing aliphatic and aromatic pendant side groups [27], and an aliphatic ether epoxy and bisphenol-A epoxy cured with amine functionalized cyclohexanes [28]. After modeling each of these systems and estimating their E_c through simulations, their data was collapsed in the same way as with the model systems and plotted in Fig. 8. The physical density of the comparison systems was not reported and if it had been the collapse of the data would most likely tighten up. As it currently is though, the data collapse together well. This is especially exciting as the yield response was correlated
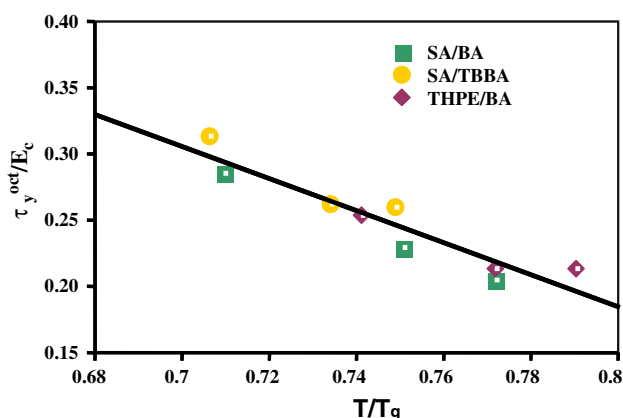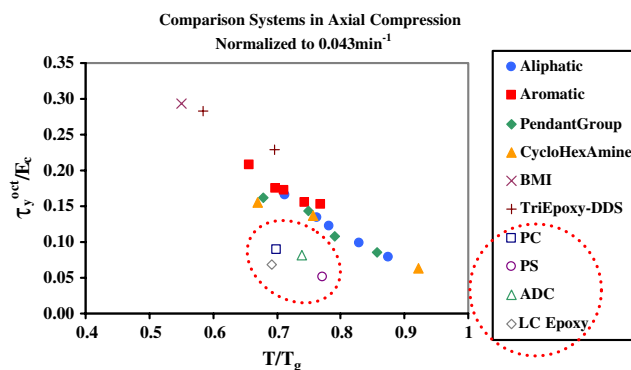
Fig. 8 The four additional molecular architectures, taken from literature sources, collapse linearly with the model aliphatic and aromatic systems. All tests were performed under uniaxial compression and 298 K with a shift in strain rate to an octahedral strain rate of 0.043 min^{-1}. The systems circled did not collapse for reasons mentioned in the discussion

reasonably well with T_g and E_c by only knowing the chemical structure and a few easily measured values. All in all, the yield behavior of nine architecturally different glassy polymer networks has now been related through T_g and E_c.

An important feature of the above four literature systems used for comparison is they all contained well-defined networks. Four additional systems that were studied for further comparisons do not fall into this category. Polystyrene (PS) and polycarbonate (PC) samples were prepared and modeled and two other systems were taken from literature; an allyl diglycol carbonate (ADC) [29] and a liquid crystalline (LC) epoxy network [30]. If these architectures are included with the other comparison systems in Fig. 8, one clearly sees they fall below the collapse of the others as highlighted by the dotted circle. This is thought to occur for a variety of reasons. The PS and PC are thermoplastics and it is well known that PC exhibits a strong β relaxation well above that of an epoxy-based network that would not be captured with the T_g alone. Both of these systems were also prepared with little attention paid to processing. The effects of orientation and thermal stresses present from processing can be quite strong in thermoplastics, more so than with thermosets. The two normalized terms do not consider processing conditions at this time. The ADC system contains a poorly defined crosslinked network due to the nature of the free radical polymerization. It appears essential to have a well-defined network for modeling purposes as with the previous systems. Finally, the LC epoxy contains a heterogeneous phase that was not accommodated for during modeling.

Fig. 7 The three phenolic extended systems, tested in plane strain at 0.02 min^{-1} and 298 K, are shown to collapse linearly also

Though the yield behavior of several systems was unable to be related through the T_g and E_c, it is still proposed these two parameters capture certain fundamental characteristics of a material that govern its yield response. The fact that several systems could not be related suggests there could be other parameters that describe the unique differences of these systems and could also be related to yielding. However, the T_g and E_c appear to be two material parameters that have a primary effect on the yield response due to what they physically represent, the network strength and stiffness. Additional parameters may not have such a primary effect on the yield response and are more secondary characteristics related to yielding.

Conclusions

The two proposed molecular parameters, T_g and E_c, quantify and are able to tolerate a variety of changes in the molecular architecture of a glassy polymer. They appear to have a primary effect on the yield behavior of the material. Characteristics such as M_c, f_c, and backbone stiffness all affect the yield response, but they do so in a collective manner seen through network stiffness. The T_g captures the overall effect of network stiffness and can be said to be a primary characteristic. The E_c is complimentary in that it captures network strength and the intermolecular interactions that contribute to it. Thus, the T_g and E_c are governing parameters of yield behavior. Both parameters are relatively easily measured or estimated and could possibly be used to predict the yield response of a polymer in previously untested conditions. As with any prediction though a certain degree of prudence needs to be used until the generality of these parameters is investigated further. Currently, they appear to be effective at relating the yield response of well-defined, glassy thermosets. This was shown by relating the yield response of various polymer networks possessing nine different molecular architectures and tested over a range of temperatures, strain rates, and two stress states. Four additional molecular architectures were unable to be related due to being thermoplastics, strong secondary relaxations not considered by T_g or E_c, orientation induced during molding, having an ill-defined network structure, and/or containing heterogeneous phases.

References

1. www.freedoniagroup.com/Epoxy-Resins-In-North-America.html
2. Sternstein SS, Ongchin L (1969) ACS Polym Prep 10:1117
3. Sultan JN, McGarry FJ (1973) Polym Eng Sci 13:29
4. Carapellucci LM, Yee AF (1986) Polym Eng Sci 26:920
5. Kinloch AJ, Young RJ (1983) Fracture behavior of polymers. Applied Science Publishers, London, pp 116–117, 172
6. Robertson RE (1966) J Chem Phys 44:3950
7. Duckett RA, Rabinowitz S, Ward IM (1970) J Mater Sci 9:909
8. Sha Y, Hui CY, Ruina A, Kramer EJ (1995) Macromolecules 28:2450
9. Baljon ARC, Robbins MO (2001) Macromolecules 34:4200
10. Chui C, Boyce MC (1999) Macromolecules 32:3795
11. Yang L, Srolovitz DJ, Yee AF (1997) J Chem Phys 107:4396
12. Rottler J, Robbins MO (2001) Phys Rev E 64:051801
13. Theodorou DN, Suter UW (1986) Macromolecules 19:139
14. Hertzberg R (1989) Deformation and fracture mechanics of engineering materials, 3rd edn. John Wiley and Sons, New York
15. Crawford E, Lesser AJ (1998) J Polym Sci Part B: Pol Phys 36:1371
16. Crawford E, Lesser AJ (1997) J Appl Polym Sci 66:387
17. Graessley WW (1975) Macromolecules 8:186
18. Flory PJ (1979) Polymer 20:1317
19. Lesser AJ, Calzia KJ (2004) J Polym Sci Part B: Pol Phys 42:2050
20. Calzia KJ, Lesser AJ (2004) Abstr Pap Am Chem Soc 227:471-PMSE Part 2
21. Calzia KJ, Lesser AJ (2004) SPE ANTEC Tech Papers, 50
22. van Krevelen DW (1976) Properties of polymers, 2nd edn. Elsevier, Amsterdam, pp 129–159
23. Allen MP, Tildesley DJ (1987) Computer simulations of liquids. Oxford University Press, Oxford
24. Kody RS, Lesser AJ (1997) J Mater Sci 32:5637
25. Donnellan TM (1992) J Polym Eng Sci 32:415
26. MacKinnon AJ (1995) J Polym Sci Part B: Pol Phys 58:2345
27. Cook WD (1999) Polymer 40:1209
28. Sindt O, Perez, J (1996) Polymer 37:2989
29. Chaplin RP (1994) Polymer 35:752
30. Ober CK, Kramer EJ (1998) Macromolecules, 31:40